Laminar Dilute Suspension Flows in Plate-and-Frame Ultrafiltration Units

A computer simulation model for suspension flows in plate-and-frame type membrane modules has been developed. Reduced forms of the mass transport and momentum equation were solved simultaneously to study concentration polarization and permeation flux decline. The verified simulator can be used to analyze and predict the process dynamics and can aid in the design of ultrafiltration systems.

CLEMENT KLEINSTREUER
and
M. S. PALLER

Department of Chemical and Environmental Engineering
Rensselaer Polytechnic Institute
Troy, NY 12181

SCOPE

Membrane separation processes are increasingly employed for purifying, concentrating and fractionating dissolved, suspended and colloidal matter from gaseous or liquid streams (Shuval, 1977; Spiegler and Laird, 1980; Cooper, 1980; Belfort, 1982). In addition, material recovery from concentrates and energy recovered from (heated) permeate streams are possible (Gaddis et al., 1979). Two common membrane filtration processes are hyperfiltration (reverse osmosis or diffusive ultrafiltration) where microsolutes are retained, and ultrafiltration (mechanical solute filtration) where dissolved species as well as suspended or colloidal particles are rejected.

A frequently used membrane unit is the plate-and-frame type module which can be represented by a parallel-plate channel with one porous wall which is the semipermeable ultrafiltration membrane. To investigate the significant transport phenomena for the case of laminar dilute suspension flow, in particular concentration polarization and permeation flux decline, a computer simulation model was developed. The equations of motion and the mass transport equation were solved using a perturbation method and a backward finite difference scheme respectively. Unique features of the system include: (1) the strong coupling of concentration polarization and permeate fluxes; (2) the asymmetry of the flow field; and (3) the fact that some of the boundary conditions are unknown *a priori* so that an iterative scheme had to be employed.

Traditionally, the convection-diffusion equation is used as the principal equation where the axial and transverse velocity profiles are obtained either from prescribed functions or a reduced form of the momentum equation. A perturbation solution of a simplified equation of motion describing laminar flow between two porous plates (or in a porous tube) and constant wall velocity (permeate flux) was given by Berman (1953). Approximate solutions of problem-specific equations were reported by Gill et al. (1965) employing a series expansion, Kozinski et al. (1970) using Bessel functions, and Leung and Probstein (1979) resorting to the integral method. The "no slip" condition is usually invoked for the longitudinal velocity at the walls; however, Beavers and Joseph (1967), Sparrow et al. (1972), Singh and Laurence (1979) and Kleinstreuer et al. (1982) investigated the effect of a thin moving layer in the porous walls. The computed or assumed velocity field is then inserted into the convection-diffusion equation to obtain the dissolved species distribution using again approximation techniques (e.g., Sherwood et al., 1965; Gill et al., 1965; Johnson and McCutchan, 1972; Hung and Tien, 1976; Leung and Probstein, 1979) or a finite difference method (e.g., Brian, 1965; Singh and Laurence, 1979). This approach is only justified if wall suction (or the transmembrane flux) does not disturb the bulk flow.

CONCLUSIONS AND SIGNIFICANCE

In practical applications of membrane separation processes, steady, optimal permeate flux cannot be maintained due to concentration polarization or membrane fouling. Concentration polarization as mainly observed in reverse osmosis modules is the boundary layer development of dissolved inorganic ions at the membrane surface. In ultrafiltration concentrated macrosolutes might form gel-layers which together with the deposition of colloidal and other large particles lead to membrane fouling. Both mass transfer phenomena and means of their reduction are strongly coupled to the fluid dynamics, or more specifically, to the transmembrane flux and the high shear stress flow of a given membrane unit (Probstein, 1972; Kleinstreuer and Belfort, 1983).

In this paper we focus on the effects of concentration polarization in an asymmetric ultrafiltration unit.

A review of the published literature indicates that, in general, the field equations for any membrane process are decoupled and drastically reduced assuming symmetric, steady, nearly unidirectional, isothermal, laminar dilute suspension flow with constant fluid and membrane properties.

The assumptions of decoupled modeling equations with constant coefficients as well as unidirectional flow and symmetrical concentration profiles were lifted for the simulation of the process dynamics of dissolved and suspended species following the fluid motion and being separated in plate-and-frame type ultrafiltration modules. The computer simulation model can be used to investigate important system parameters and transport mechanisms towards optimal process design. Results of specific computer simulation studies compare favorably with experimental observations published by Madsen (1977).

Correspondence concerning this paper should be directed to C. Kleinstreuer.

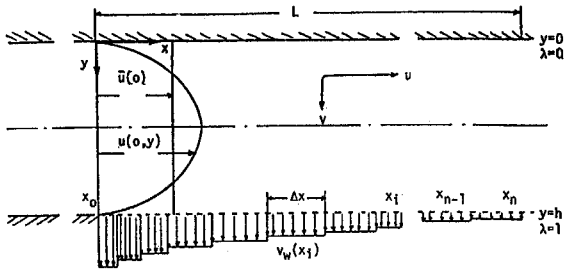

Figure 1. Coordinate system and segmentation of plate-frame membrane unit into *n* permeable-walled subchannels.

MODEL DESCRIPTION

Modeling Approach

The system discussed in this paper is a plate-and-frame type ultrafiltration module which can be conceptualized as a parallel-plate channel with one porous wall (Figure 1). The unique features of interest include: (1) the asymmetry of the flow field; (2) the coupling of concentration polarization and transmembrane fluxes; and (3) the unknown conditions at the porous wall for solute concentration and normal velocity component.

Other systems (e.g., tubular or two-sided channel membranes) could be accommodated with a simple coordinate transformation and a modification of the boundary conditions. We assume steady, two-dimensional, laminar flow without external forces and entrance or end effects. The fluid properties are constant and the solute is convected by the carrier fluid. The channel of length L is subdivided into n segments to study the effect of local parameter dependencies, in particular the variability of the permeate flux v_w with bulk velocity distributions and concentration boundary layer developments. Hence the momentum and mass transport equations are coupled via the wall velocity v_w plus the solute concentration at the wall c_w, and they have to be solved simultaneously. The suction velocity v_w is mainly a function of the deposition layer thickness and permeability as well as hydraulic membrane characteristics. It is kept constant within the subregions $\Delta x = x_{i+1} - x_i$ so that $v_w(x)$ becomes actually a discrete function $v_w(x_i)$. Matching between each channel section Δx is achieved with an integrated fluid mass balance at the stations $i = 0,1,2,\ldots,n$.

Modeling Equations

The listed assumptions justify the postulates $u = u(x,y)$, $v = v(y)$ and $w = 0$ so that the continuity and Navier-Stokes equation can be reduced to (Figure 1):

$$\text{(continuity)} \qquad \frac{\partial u}{\partial x} + \frac{1}{h}\frac{\partial v}{\partial \lambda} = 0 \tag{1a}$$

$$(x\text{-momentum})\; u\frac{\partial u}{\partial x} + \frac{v}{h}\frac{\partial u}{\partial \lambda} = -\frac{1}{\rho}\frac{\partial p}{\partial x} + \nu\left(\frac{\partial^2 u}{\partial x^2} + \frac{1}{h^2}\frac{\partial^2 u}{\partial \lambda^2}\right) \tag{1b}$$

$$(y\text{-momentum}) \qquad \frac{v}{h}\frac{\partial v}{\partial \lambda} = -\frac{1}{\rho h}\frac{\partial p}{\partial \lambda} + \frac{\nu}{h^2}\frac{\partial^2 v}{\partial \lambda^2} \tag{1c}$$

The associated boundary conditions are

$$u(\lambda = 0) = 0 \text{ and } v(\lambda = 0) = 0;\quad u(\lambda = 1) = 0 \text{ and } v(\lambda = 1) = v_w \tag{1d}$$

A parabolic velocity profile is assumed for $u(x = 0,\lambda)$ at the channel "entrance." Following Berman (1953), an appropriate stream function $\psi(x,y)$ is postulated to reduce the system (Eq. 1) to an ordinary differential equation:

$$\psi(x,\lambda) = [h\bar{u}(x_i) - v_w x]f(\lambda) \tag{2}$$

where $\partial\psi/\partial\lambda = hu$, $\partial\psi/\partial x = -v$. The matching equation reflecting an integrated mass balance reads

$$A_c\bar{u}(x_i) = A_c\int_o^1 u(x_i,\lambda)d\lambda - \frac{A_w}{\Delta x}\int_{x_i}^{x_{i+1}} v_w(x_i)dx, \qquad i = 0,1,2,\ldots,n. \tag{3}$$

where A_c is the channel cross sectional area and A_w is the porous wall (membrane) area. Hence,

$$u(x,\lambda) = \left[\bar{u}(x_i) - v_w\frac{x}{h}\right]f'(\lambda) \tag{4a}$$

$$v(\lambda) = v_w f(\lambda). \tag{4b}$$

Cross differentiation of Eqs. 1b and 1c and subtracting one resulting equation from the other eliminates the pressure terms and insertion of Eq. 2 yields:

$$\frac{d}{d\lambda}\left[\frac{v_w}{h}\left(f'^2 - ff'' + \frac{\nu}{h^2}f'''\right)\right] = 0. \tag{5}$$

Upon integration and formation of the dimensionless group $v_w h/\nu = Re_w$ we obtain

$$Re_w(f'^2 - ff'') + f''' = C \tag{6a}$$

where the wall Reynolds number $Re_w \approx 10^{-1}$ to 10^{-2} for ultrafiltration and $Re_w \approx 10^{-3}$ for reverse osmosis operations (Belfort 1982); C is an integration constant. The associated boundary conditions are

$$\lambda = 0\text{: } f' = f = 0;\ \lambda = 1\text{: } f' = 0 \text{ and } f = 1 \tag{6b}$$

The fact that $Re_w < 1$ makes a perturbation solution possible (Berman, 1953; Van Dyke, 1975; Singh and Laurence, 1979). Hence, the velocity field is approximated by (Green, 1979):

$$u(x,\lambda) = \left[\bar{u}(x_i) - \frac{x}{h}v_w(x_i)\right]\left[6\lambda - 6\lambda^2 + \frac{Re_w}{70}(-32\lambda + 81\lambda^2 - 105\lambda^4 + 84\lambda^5 - 28\lambda^6)\right] \tag{7a}$$

$$v(x,\lambda) = v_w(x_i)\left[3\lambda^2 - 2\lambda^3 + \frac{Re_w}{70}(-16\lambda^2 + 27\lambda^3 - 21\lambda^5 + 14\lambda^6 - 4\lambda^7)\right] \tag{7b}$$

Inserting the solutions (Eqs. 7a and 7b) into the governing equations (Eqs. 1b and 1c) yields the pressure distribution as

$$p(x,\lambda) = p(0,0) - \frac{\rho}{2}v_w{}^2[f(\lambda)]^2 + \frac{\mu v_w}{h}f'(\lambda) + \frac{\mu C}{h}\left[\bar{u}(x_i)x - \frac{x^2}{2h}v_w\right]. \tag{7c}$$

Numerical expressions for $f(\lambda)$, $f'(\lambda)$ and C were obtained by solving the system (Eq. 6). Submodels for the permeate volume flux or wall velocity v_w are usually based on Darcy's law and advancements made by Kedem and Katchalsky (1958) and Merten (1963):

$$v_w = k(\Delta p - \Delta\pi) \tag{8a}$$

Various authors developed expressions for the permeability coefficient k, the driving pressure drop Δp and the osmotic pressure difference $\Delta\pi$ depending upon the availability of measured and/or computed parameters (e.g., Brian, 1966; Sherwood et al., 1967; Blatt et al., 1970; Dandavati et al., 1975; Hung and Tien, 1976; Leung and Probstein, 1979; Kabadi et al., 1979).
We follow a semiempirical approach so that

$$v_w(x_i) = k_{\text{eff}}^i[\Delta p(x_i,\lambda = 1) - \pi(c_w)];\quad i = 0,1,\ldots,n \tag{8b}$$

where k_{eff}^i is the *local* effective permeability of the deposition/membrane layer, within each segment; Δp can be obtained from Eq. 7c; the osmotic pressure on the feed side π is a function of the constituent concentration near the wall and could be obtained from a $\pi(c)$-chart (e.g., Leung and Probstein, 1979). Before Eq. 7 can be evaluated, the solute concentration distribution has to be com-

TABLE 1. INPUT-DATA FOR FIGURES 2–4 (SOLUTION: BOVINE SERUM ALBUMIN IN 0.15 M SALINE WATER AT pH = 4.7)

Channel Length	$L = 48$ cm
Channel Height	$h = 0.38$ cm
Average Inlet Veloc.	$\bar{u}_o = 34.56$ cm/s
Max. Permeate Veloc.	$v_{wo} = 0.5 \times 10^{-3}$ cm/s
Appl. Pressure	$\Delta p = 0.1 \times 10^6$ Pa
Initial Diffusion	$D_o = 0.35 \times 10^{-5}$ cm^2/s
Initial Concentr.	$C_o = 1.65$ g/100 cm^3
Membrane Permeab.	$k_o = 0.5 \times 10^{-8}$ cm^3/(cm^2·s·Pa)

puted.

The mass transport (or transient convection-diffusion) equation can be modified for our case study to

$$u\frac{\partial c}{\partial x} + v\frac{\partial c}{\partial \lambda} = a_i\frac{\partial^2 c}{\partial \lambda^2} + S \qquad (9a)$$

where $u = \dfrac{\tilde{u}}{u(0)}$, $v = \dfrac{\tilde{v}}{v_w(0)}$, $c = \dfrac{\tilde{c}}{c_o}$,

$$x = \frac{\tilde{x}}{L},\ \lambda = \frac{\tilde{y}}{h} \text{ and } a_i = \frac{D^t}{\tilde{v}_w(x_i)h}.$$

D^t is the local effective mean diffusion coefficient and S the net sink of constituent c in cases where some solute material permeates through the membrane. The associated boundary conditions are

- "initial" condition $c(0,\lambda) = 1$
- at the membrane wall $a_i\left.\dfrac{\partial c}{\partial \lambda}\right|_{\lambda=1} = rc(x,1)$ (9b)
- at impermeable wall $a_i\left.\dfrac{\partial c}{\partial \lambda}\right|_{\lambda=0} = 0.$

For a membrane of 100% solute-rejection efficiency, $r = 1$ and $S = 0$. The systems of Eqs. 7, 8c and 9 together with the empirical relationships for $\pi(c)$ and $D(c)$ (taken from Leung and Probstein, 1979) were programmed on an IBM 3033 using a backward finite differencing scheme (Roache, 1976) for solving Eq. 9a. The grid spacing in y-direction was very fine near the membrane surface and was relaxed towards the channel centerline. Strong deviations from a mesh of *smoothly* varying density caused (local) instabilities. The unique features of the system (e.g., asymmetry and unknown boundary conditions) required a special matrix equation solver plus an iterative scheme to find the true solute concentration at the membrane c_w in order to compute the true v_w where in turn $v_w = v_w(c_w)$.

SIMULATION RESULTS AND DISCUSSIONS

Results and Discussions

The hydrodynamic aspects of the asymmetric system can be best described in contrasting the maximum axial velocity, the transverse velocity, and the wall shear rates to the symmetric case (Berman, 1953). The deviation of the maximum axial velocity from the centerline can be obtained by setting the derivative of Eq. 7a to zero and solving for $\lambda(Re_w)$. A trial and error solution yields $\lambda_m(Re_w = 1.0) = 0.52$; i.e. a maximum deflection of 4% occurs. The shear stresses at the walls are directly affected by the skewed axial velocity profiles. The shear rate is greater than for Poiseuille flow at the porous wall ($\lambda = 1$) and less at the solid wall ($\lambda = 0$). The ratio of wall shear stresses between the plate-and-frame system and a Poiseuille flow system is 1.095; i.e., shear stresses at the membrane are up to 9.5% higher than in the case of zero suction. The transverse velocity distribution (Figure 2) differs of course significantly from the corresponding velocity field of a symmetric membrane module. Since solute is primarily transported towards the membrane by convection, an accurate evaluation of the flow field is most important. Table 1 lists the basic input data used for the computer simulation runs shown in Figures 2 to 4. The geometric and operational input data were, for the most part, extracted from Leung and Probstein (1979).

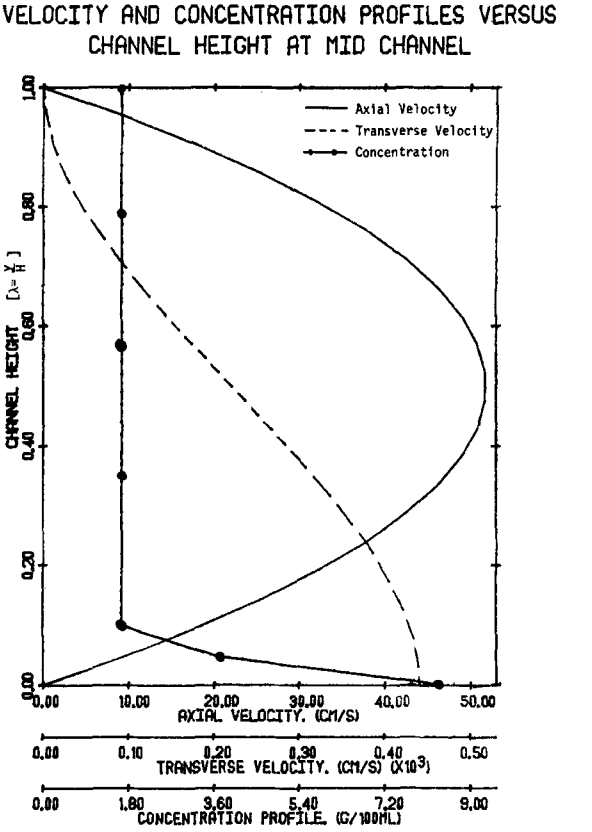

Figure 2. Velocity distributions and concentration profile vs. channel height at midchannel.

Figure 2 shows in addition to the axial and transverse velocity distributions, the steady-state concentration profile at midchannel with $c_{bulk} \approx 1.65$ g/100 mL and $c_{wall} \approx 8.6$ g/100 mL. The concentration boundary-layer occupies about 8% of the channel height. Figure 3 depicts the typical flux decline with channel length as similarly predicted by other researchers. At high Peclet numbers solute is rapidly convected to the membrane wall which reduces the permeate flux in the first quarter of the membrane significantly (Eq. 8a). During this process, convective mass flux and back diffusion of solute into the bulk flow are in dynamic equilibrium at any point along the membrane wall [B.C. (Eq. 9b)]. Figure 4 shows the undesirable effect of solute build-up as concentration polar-

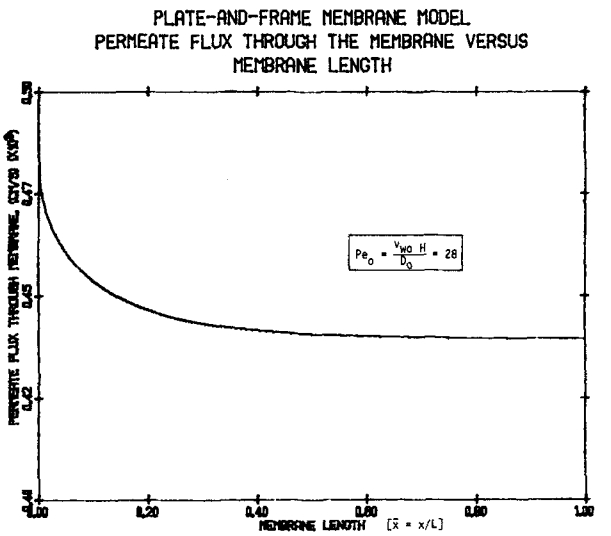

Figure 3. Permeate flux along membrane wall.

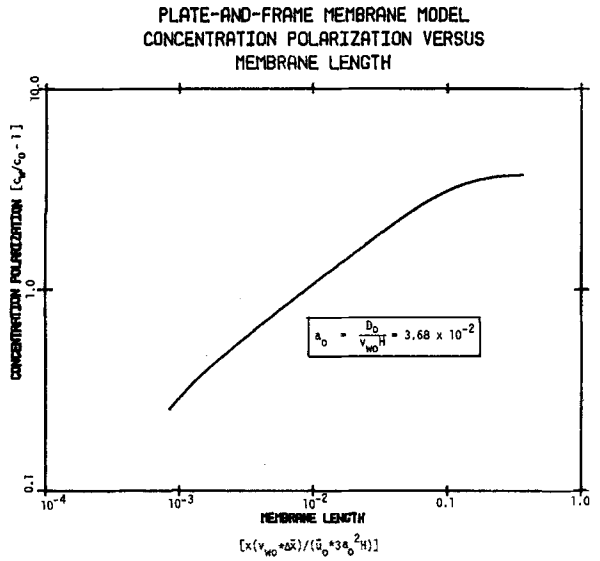

Figure 4. Development of concentration polarization.

ization at a high Peclet number vs. a nondimensionalized membrane length. This plot is the counterpart to the graph introduced by Sherwood et al. (1965) for desalination with reverse osmosis membranes.

Figure 5 with the associated input data given in Table 2 depicts an application of the simulator to a pilot-plant test case of whey separation using a plate-and-frame ultrafiltration module by Madsen (1977, p. 50, Fig. 3.6). It has to be noted that information on the functional forms and values of key parameters is scarce. For example, no "initial" (or entrance) conditions are described and expressions for the diffusivity and osmotic pressure of whey had to be obtained elsewhere (Sourirajan, 1977). The effective *local* membrane permeability, k'_{eff} of Eq. 8b was deduced from the measured pure water flux which explains the similar trend between pure water flux, observed flux decline, and computer prediction. The unusual behavior of the pure water flux curve is due to the particular properties of the ultrafiltration membrane used in the plate-and-frame test unit built by Madsen (1977). The simulator predicts at the beginning of the membrane channel a sharp flux decline as expected and documented in Figure 5 as well as in Figure 3 for a different constituent. Due to the enhanced membrane permeability, the permeation flux increases and predicted and measured permeate flux values agree very favorably. The initial discrepancy between observed and predicted data points may be caused by entrance effects. For example, according to the experiment, the initial membrane flux for the given applied pressure difference and volumetric flow rate is maintained in the first 10 cm of the module before a "moderate" flux decline occurs (dashed line segment in Figure 5). Madsen (1977) does not give any rationale for this unusual behavior of the permeate flux curve. In contrast, the modeling study indicates an immediate drop in permeate flux due to strong initial build-up of solute at the membrane. The simulator was also used for sensitivity analyses of other typical dependencies such as channel geometry, applied pressure drop, axial inlet velocity and "slip" condition at the membrane surface (Kleinstreuer et al., 1982).

CONCLUSIONS AND FUTURE WORK

A computer simulation model for dilute suspension flow in a plate-and-frame membrane module is discussed. Special emphasis is placed on the effects of the asymmetric flow field on solute transfer to the membrane surface during steady state ultrafiltration.

Although predictive computer simulation models for (laminar) boundary-layer type suspension flows in parallel-plate or tubular membrane units exist, their application is restricted to specific types

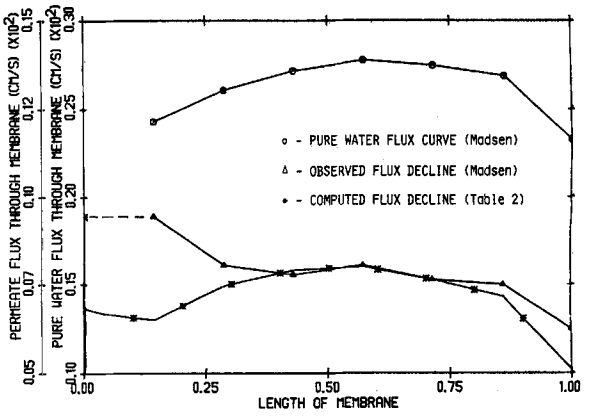

Figure 5. Comparison of observed and predicted data for flux decline.

TABLE 2. INPUT DATA FOR FIGURE 5 (SOLUTION: WHEY WITH TOTAL SOLID CONCENTRATION OF 6.2% AT pH = 5.0)

Channel Length	$L = 70.0$ cm
Channel Height	$h = 0.10$ cm
Initial Axial Mean Veloc.	$\bar{u}_o = 100.0$ cm/s
Initial Transverse Veloc.	$v_{wo} = 9.44 \times 10^{-4}$ cm/s
Pressure Difference	$\Delta p = 4.0 \times 10^5$ Pa
Initial Diffusivity	$D_o = 2.628 \times 10^{-6}$ cm^2/s
Initial Concentration	$C_o = 2.2$ g/100 cm^3
Initial Membrane Permeability	$k_o = 2.36 \times 10^{-9}$ cm/Pa·s
Kinematic Viscosity	$\nu = 0.0198$ St

of solutes, flow patterns and membranes. Hence, one basic research task is to develop a flexible, comprehensive model which is capable of simulating in detail the dynamic interactions of various solutes and their distributions with the carrier fluid, the laminar/turbulent flow patterns, and the sieve or diffusive type membranes. For example, reverse osmosis and ultrafiltration processes are, for all practical purposes, time-dependent and prone to membrane fouling. Future work should concentrate on modeling these characteristics accurately.

ACKNOWLEDGMENT

The authors would like to thank G. A. Green for assistance.

NOTATION

a = inverse Peclet number
A = area
c = solute concentration
D = diffusion coefficient
f = similarity function
h,H = channel height
k = membrane permeability
L = channel length
p = pressure
Pe = Peclet number
S = sink or source of solvent
r = solute rejection coefficient
Re = Reynolds number
u = axial velocity
v = transverse velocity
x = longitudinal coordinate
y = normal coordinate (Figure 1)

Greek Letters

Δ = difference
λ = nondimensional normal coordinate

μ = dynamic viscosity of solvent
μ = kinematic viscosity of solvent
ρ = density of solvent
ψ = stream function
π = osmotic pressure

Subscripts

c = channel
eff = effective
i = counter; $i = 0,1,2,\ldots,n$
m = maximum
o = "initial" (or entrance) condition
w = membrane wall

Superscripts

$\bar{f}$ = average of variable f, nondimensionalized value of f
$\tilde{f}$ = dimensional value of f
i = counter; $i = 0,1,2,\ldots,n$

LITERATURE CITED

Beavers, G. S., and D. D. Joseph, "Boundary Conditions at a Naturally Permeable Wall," *J. Fluid Mech.*, **30**, p. 197 (1967).

Belfort, G., Eds., Membrane Methods in Water and Wastewater Treatment," Academic Press, New York (1982).

Berman, A. S., "Laminar Flow in Channels with Porous Walls," *J. Appl. Phys.*, **24**, p. 1232 (1953).

Blatt, W. F., A. Dravid, A. S. Michaels, and L. Nelson, "Membrane Science and Technology," J. E. Flinn, ed., Plenum Press, New York (1970).

Brian, P. L. T., "Concentration Polarization in Reverse Osmosis Desalination with Variable Flux and Incomplete Salt Rejection," *I & EC Fund.*, **4**, p. 439 (1965).

——, "Desalination by Reverse Osmosis," M.I.T. Press, U. Merten, ed. (1966).

Cooper, A. R., ed., "Ultrafiltration Membranes and Applications," Polymer Science and Techn., **13**, Plenum Press, New York (1980).

Dandavati, M. S., M. R. Doshi, and W. N. Gill, "Hollow Fiber Reverse Osmosis: Experiments and Analysis of Radial Flow Systems," *Chem. Eng. Sci.*, **30**, p. 877 (1975).

Gaddis, J. L., C. A. Brandon, and J. J. Porter, "Energy Conservation Through Point Source Recycle with High Temperature Hyperfiltration," EPA Report No. EPA-600/7-79-131 (1979).

Gill, W. N., C. Tien, and D. W. Zeh, "Concentration Polarization Effects in a Reverse Osmosis System," *I & EC Fund.*, **4**, p. 433 (1965).

Green, G. A., "Laminar Flow Through a Channel with One Porous Wall," Course Project in Adv. F.M., Dept. of Chem. & Env. Eng., RPI, Troy, NY (1979).

Hung, C. C., and C. Tien, "Effect of Particle Deposition on the Reduction of Water Flux in Reverse Osmosis," *Desalination*, **18**, p. 173 (1976).

Johnson, J. S., and J. W. McCutchan, "Concentration Polarization in the Reverse Osmosis Desalination of Sea Water," *Desalination*, **10**, p. 147 (1972).

Kabadi, V. N., M. R. Doshi, and W. N. Gill, "Radial Flow Hollow Fiber Reverse Osmosis: Experiments and Theory," *Chem. Eng. Commun.*, **3**, p. 339 (1979).

Kedem, O., and A. Katchalsky, "Thermodynamic Analysis of the Permeability of Biological Membranes to Non-Electrolytes," *Biochimica et Biophysica Acta*, **27**, p. 229 (1958).

Kleinstreuer, C., and M. R. Patterson, FLUOMEG, ORNL-TM 7115, Oak Ridge National Lab., Oak Ridge, TN (1980).

Kleinstreuer, C., "Mathematical Modeling of Engineering Systems," Wiley-Interscience, New York (in preparation).

——, and G. Belfort, "Membrane Methods in Water and Wastewater Treatment," G. Belfort, ed., Academic Press, New York (1983).

——, M. S. Paller, and T. P. Chin, "Modeling of Engineering Systems," **II**, W. E. Ames, ed., North-Holland Publ. Corp., Amsterdam, The Netherlands (1982).

Kozinski, A. A., F. P. Schmidt, and E. N. Lightfoot, "Velocity Profiles in Porous-Walled Ducts," *Ind. Eng. Chem. Fund.*, **9**, p. 502 (1970).

Leung, W. F., and R. F. Probstein, "Low Polarization in Laminar Ultrafiltration of Macromolecular Solutions," *Ind. Eng. Chem. Fund.*, **18**, p. 274 (1979).

Madsen, R. F., "Ultrafiltration in Plate-and-Frame Type Membrane Units," Elsevier Publ. Co., Amsterdam (1977).

Merten, U., "Flow Relationships in Reverse Osmosis," *I & EC Fund.*, **2**, p. 229 (1963).

Probstein, R. F., "Desalination: Some Fluid Mechanical Problems," A Freeman Scholar Lecture, *Trans. ASME, J. Basic Eng.* (June, 1972).

Roache, P. J., "Computational Fluid Dynamics," Hermosa Publ., New York (1976).

Sherwood, T. K., P. L. T. Brian, R. E. Fisher, and L. Dresner, "Salt Concentration at Phase Boundaries in Desalination by Reverse Osmosis," *I & EC Fund.*, **4**, p. 113 (1965).

Shuval, H. I., ed., "Water Renovation and Reuse," Academic Press, New York (1977).

Singh, R., and R. L. Laurence, "Influence of Slip Velocity at a Membrane Surface on Ultrafiltration Performance: I. Channel Flow System," *Int. J. Heat Mass Transfer*, **22**, p. 721 (1979).

Sourirajan, S., "Reverse Osmosis and Synthetic Membranes," National Research Council of Canada, NRCC No. 15627, Ottawa, Canada (1977).

Sparrow, E. M., V. K. Jonsson, G. S. Beavers, and R. G. Owen, "Incompressible Turbulent Flow in a Permeable-Walled Duct," *Trans. ASME, J. Basic Eng.*, 314–320 (1972).

Spiegler, K. S., and A. D. K. Laird, eds., "Principle of Desalination," Academic Press, New York (1980).

Van Dyke, M., "Perturbation Methods in Fluid Mechanics," The Parabolic Press (1975).

Manuscript received July 24, 1981; revision received August 24, and accepted September 3, 1982.